The Canadian Mineralogist
Vol. 37, pp. 1483-1491 (1999)

THE STRUCTURE OF MASUYITE, $Pb[(UO_2)_3O_3(OH)_2](H_2O)_3$, AND ITS RELATIONSHIP TO PROTASITE

PETER C. BURNS[§] AND JOHN M. HANCHAR

Department of Civil Engineering and Geological Sciences, University of Notre Dame, 156 Fitzpatrick Hall, Notre Dame, Indiana 46556, U.S.A.

ABSTRACT

The structure of masuyite, $Pb[(UO_2)_3O_3(OH)_2](H_2O)_3$, $Z = 2$, monoclinic, a 12.241(3), b 7.008(2), c 6.983(2) Å, β 90.402(4)°, space group *Pn*, has been solved by direct methods and refined by full-matrix least-squares techniques to an agreement index (R) of 6.3% for 2473 unique observed reflections ($|F_o| \geq 4\sigma_F$) collected using Mo$K\alpha$ X-radiation and a CCD-based area detector. The structure contains three symmetrically distinct U^{6+} positions, each of which is occupied by nearly linear $(UO_2)^{2+}$ uranyl ions (*Ur*) that are coordinated by five additional anions arranged at the equatorial corners of pentagonal bipyramids capped by the O_{Ur} anions. The uranyl pentagonal bipyramids share edges to form α-U_3O_8-type sheets that are parallel to (010). The interlayer contains two distinct Pb^{2+} sites as well as three H_2O groups. The Pb(1) site is close to fully occupied and is coordinated by seven atoms of O that are contained in the sheets of uranyl polyhedra, and three H_2O groups. The Pb(2) site is only ~12% occupied and is coordinated by six atoms of O from the sheets of uranyl polyhedra and three H_2O groups. The structure of masuyite is closely related to that of protasite, but has an additional cation site in the interlayer.

Keywords: masuyite, uranyl mineral, protasite, structure determination.

SOMMAIRE

Nous avons résolu la structure de la masuyite, $Pb[(UO_2)_3O_3(OH)_2](H_2O)_3$, $Z = 2$, monoclinique, a 12.241(3), b 7.008(2), c 6.983(2) Å, β 90.402(4)°, groupe spatial *Pn*, par méthodes directes sur matrice entière par moindres carrés jusqu'à un résidu R de 6.3% en utilisant 2473 réflexions uniques observées ($|F_o| \geq 4\sigma_F$) avec rayonnement Mo$K\alpha$ et mesurées avec un détecteur à aire de type CCD. La structure contient trois positions U^{6+} symétriquement distinctes, occupées dans chaque cas par un groupe uranyle $(UO_2)^{2+}$ presque linéaire (*Ur*) auquel sont coordonnés cinq anions additionels disposés aux coins équatoriaux de dipyramides pentagonales ayant comme terminaison les anions O_{Ur}. Les bipyramides pentagonales à uranyle partagent des arêtes pour former des feuillets de type α-U_3O_8 parallèles à (010). L'interfeuillet contient deux sites Pb^{2+} distincts, de même que trois sites H_2O. Le site Pb(1) est près d'être plein, et est en coordinence avec sept atomes d'oxygène qui font partie des feuillets de polyèdres à uranyle, et trois groupes H_2O. En revanche, le site Pb(2) n'est que partiellement occupé (~12%); les liaisons proviennent de six atomes d'oxygène des feuillets de polyèdres à uranyle et trois groupes H_2O. La structure de la masuyite partage plusieurs points communs avec celle de la protasite, mais elle possède un site cationique additionnel entre les feuillets.

(Traduit par la Rédaction)

Mots-clés: masuyite, minéral à uranyle, protasite, détermination de la structure.

INTRODUCTION

The complex paragenesis of low-temperature uranyl minerals, especially Pb uranyl oxide hydrates, challenges our understanding of mineralogy. The Pb uranyl oxide hydrates are important to an understanding of the genesis of geologically old deposits of uranium, where they occur in abundance in the oxidized portions owing to the presence of substantial radiogenic Pb (Frondel 1958). Knowledge of the occurrences and crystal chemistry of these minerals has lagged behind many other mineral groups owing to extreme experimental difficulties associated with the determination of their structures. Pb uranyl oxide hydrates seldom occur as crystals of suitable size for structure analysis, generally are twinned, commonly possess pseudosymmetry and unusually large unit-cells, and are extreme absorbers of X-rays.

As part of ongoing research into the crystal chemistry of uranyl minerals, several specimens of masuyite

§ *E-mail address*: pburns@nd.edu

were obtained, and crystals of suitable size and quality for a crystal-structure determination were sought. Only one such crystal has been found, for which chemical analysis indicate a Pb:U ratio of ~1:3; details of the structure are reported herein.

Background Information

The seven Pb uranyl oxide hydrate minerals are listed, together with their chemical formulae and selected crystallographic parameters, in Table 1. The recent introduction of CCD-based detectors of X-rays in mineralogical research (Burns 1998a) has permitted the elucidation of the structures of wölsendorfite (Burns 1999), richetite (Burns 1998b), and vandendriesscheite (Burns 1997). It has been shown that each Pb uranyl oxide hydrate structure is based upon complex sheets of edge- and corner-sharing uranyl polyhedra (Fig. 1), with the uranyl ions oriented roughly perpendicular to the sheets, and with Pb^{2+} cations and H_2O groups located in the interlayers between the sheets. Some of the sheets of uranyl polyhedra are unique to Pb uranyl oxide hydrates, whereas others occur in other uranyl phases. The fourmarierite-type sheet (Fig. 1c) also occurs in schoepite (Finch *et al.* 1996), and the richetite-type sheet (Fig. 1d) occurs in becquerelite (Pagoaga *et al.* 1987), compreignacite (Burns 1998c), billietite (Pagoaga *et al.* 1987), and protasite (Pagoaga *et al.* 1987). The curite-type sheet (Fig. 1a) is not known from another mineral, but it does occur in the structure of its synthetic Sr analogue (Burns & Hill 2000). The sayrite-type sheet (Fig. 1b) was first found in the structure of the chemical compound $K_2[(UO_2)_5O_8](UO_2)_2$ (Kovba 1972), and later in sayrite. Neither the vandendriesscheite-type (Fig. 1f) nor wölsendorfite-type (Fig. 1e) sheets have been found in any another structure, and both are extraordinarily complex; they are more complex than any other known sheet of uranyl polyhedra, either in a mineral or a synthetic phase.

Vaes (1947) described masuyite as a Pb uranyl oxide hydrate, whereas the analytical data reported for masuyite by Frondel (1958) did not contain Pb, and probably pertained to another mineral, as suggested by the reported unit-cell dimensions, which are in agreement with those of becquerelite. Brasseur (1950) presented chemical data for masuyite, with a Pb:U ratio of ~1:3. Christ & Clark (1960) obtained crystallographic data that indicate an unusually large unit-cell (*a* 41.93, *b* 24.22, *c* 42.61 Å), although it is possible that their findings were an artifact of twinning. Modern mineralogical research on masuyite has resulted in considerable confusion as to the chemical composition of the species. Deliens *et al.* (1981) provided two compositions for masuyite, one with a Pb:U ratio of ~1:3 and the other with Pb:U ~ 4:9. Finch & Ewing (1991) postulated that there may be three natural compositions that are referred to as masuyite; "masuyite I" with Pb:U ~ 1:3, "masuyite II" with Pb:U ~ 2:5, and "masuyite III" with Pb:U ~ 4:11. Finch & Ewing (1992a) found a phase resembling masuyite with a Pb:U ratio of ~1:3 as an alteration product of vandendriesscheite. Finch & Ewing (1992b) noted that "masuyite I" corresponds to the Pb analogue of protasite, $Ba[(UO_2)_3O_3(OH)_2](H_2O)_3$. Most recently, Deliens & Piret (1996) reported analytical results for 16 crystals of masuyite, and noted that they clustered on the basis of Pb:U ratios into groups with ~1:3 and ~4:9. Thus, it is apparent that two, possibly three distinct species have been referred to as masuyite in the literature.

Experimental Methods

X-ray diffraction

The specimen containing the masuyite studied forms part of the Canadian Museum of Nature collection [CMN MC 81093] and is from the Shinkolobwe uranium mine, Shaba Province, Democratic Republic of Congo. Several crystals obtained from the specimen were fragmented and examined optically, and a small blocky crystal with sharp extinction and uniform optical properties was selected for the X-ray study. The crystal, with dimensions 0.05 × 0.06 × 0.16 mm, was mounted on a Bruker PLATFORM 3-circle goniometer equipped with a 1K SMART CCD (charge-coupled device) detector and a crystal-to-detector distance of 5 cm. Burns (1998a) discussed the application of CCD detectors to the analysis of mineral structures.

The data were collected using monochromatic Mo*K*α X-radiation and frame widths of 0.3° in ω, with

TABLE 1. LEAD URANYL OXIDE HYDRATE MINERALS

		S.G.	*a* (Å)	*b* (Å)	*c* (Å)	α (°)	β (°)	γ (°)	Ref
wölsendorfite	$Pb_{6.16}Ba_{0.36}[(UO_2)_{14}O_{19}(OH)_4](H_2O)_{12}$	*Cmcm*	14.131	13.885	55.969				1
sayrite	$Pb_2[(UO_2)_5O_6(OH)_2](H_2O)_4$	$P2_1/c$	10.704	6.960	14.533		116.81		2
curite	$Pb_3[(UO_2)_8O_8(OH)_6](H_2O)_3$	*Pnam*	12.551	13.003	8.390				3
fourmarierite	$Pb[(UO_2)_4O_3(OH)_4](H_2O)_4$	$Bb2_1m$	13.986	16.400	14.293				4
richetite	$(Fe,Mg)_xPb_{8.57}[(UO_2)_{18}O_{18}(OH)_{12}]_2(H_2O)_{41}$	*P*1	20.9391	12.1000	16.3450	103.87	115.37	90.27	5
vandendriesscheite	$Pb_{1.57}[(UO_2)_{10}O_6(OH)_{11}](H_2O)_{11}$	*Pbca*	14.1165	41.478	14.5347				6
masuyite	$Pb[(UO_2)_3O_3(OH)_2](H_2O)_3$	*Pn*	12.241	7.008	6.983		90.402		

Ref: 1: Burns (1999); 2: Piret *et al.* (1983); 3: Taylor *et al.* (1981); 4: Piret (1985); 5: Burns (1998b); 6: Burns (1997).

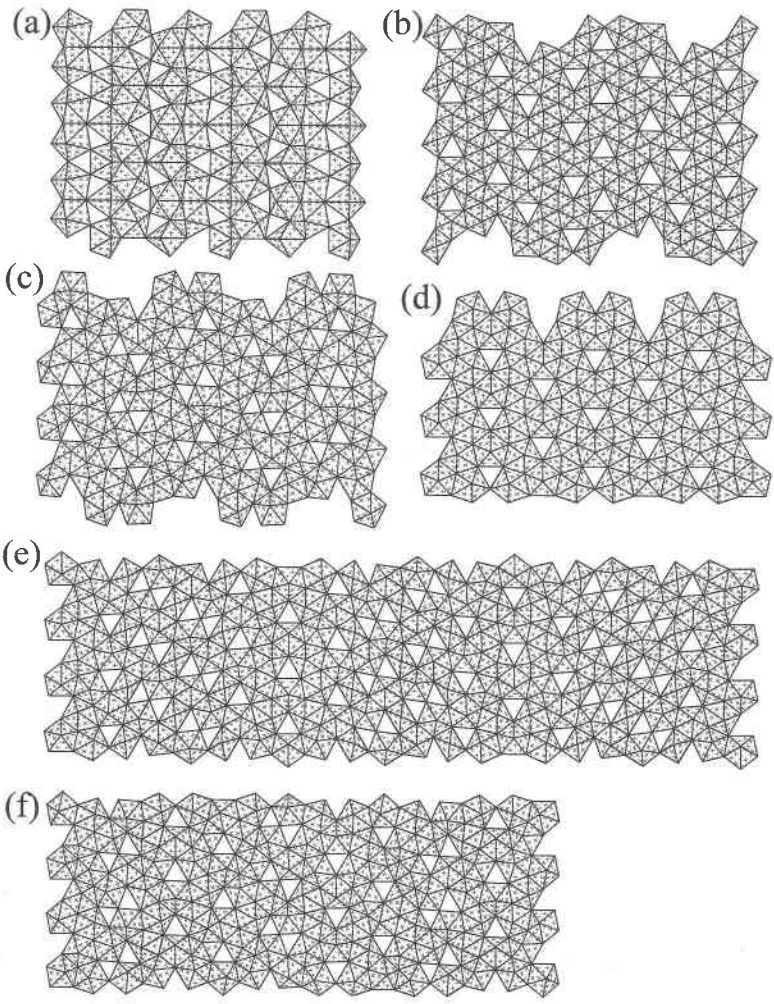

FIG. 1. Sheets of uranyl polyhedra that occur in the structures of Pb uranyl oxide hydrate minerals: (a) curite, (b) sayrite, (c) fourmarierite, (d) richetite and masuyite, (e) wölsendorfite, (f) vandendriesscheite.

60 s used to acquire each frame. A sphere of three-dimensional data was collected to ~57° 2θ. The final unit-cell dimensions (Table 2) were refined on the basis of 3862 reflections using least-squares techniques. Data were collected for $3° < 2\theta < 56.7°$ in approximately 44 hours; comparison of the intensities of equivalent reflections collected at different times during the data collection showed no evidence of significant decay. The three-dimensional data were reduced and corrected for Lorentz, polarization, and background effects using the Bruker program SAINT. An empirical absorption-correction was done using the program SADABS (G. Sheldrick, unpubl. computer program) on the basis of the intensities of equivalent reflections. A total of 6862 reflections were collected, and merging of equivalent reflections gave 2768 unique reflections (R_{INT} = 5.3%, after correction for absorption) with 2473 classed as observed ($|F_o| \geq 4\sigma_F$).

Chemical composition

A single crystal of masuyite, from the same specimen as the crystal used for the collection of the X-ray diffraction data, was mounted in epoxy, polished to half its thickness, and coated with carbon. *In situ* chemical analyses were done in wavelength-dispersion spectroscopy (WDS) mode on a JEOL 8600 electron microprobe at the University of Western Ontario. Data reduction

TABLE 2. MISCELLANEOUS INFORMATION PERTAINING TO THE STRUCTURE REFINEMENT OF MASUYITE

a (Å)	12.241(3)	Crystal size (mm)	0.16x0.06
b (Å)	7.008(2)		x0.05
c (Å)	6.983(2)	Total ref.	6862
β (°)	90.402(4)	Unique ref.	2769
V (Å^3)	599.0(1)	R_{int} (%)	5.3
Space group	Pn	Unique $\|F_o\| \geq 4\sigma_F$	2473
F(000)	956	Final R (%)	6.3
μ (mm^{-1})	54.5	S	1.12
D_{calc} (g/cm^3)	6.394		

Unit-cell contents: $2\{Pb[(UO_2)_3O_3(OH)_2](H_2O)_3\}$

$R = \Sigma(|F_o|-|F_c|)/\Sigma|F_o| \times 100$

$S = [\Sigma w(|F_o|-|F_c|)^2/(m-n)]^{1/2}$, for m observations and n parameters

TABLE 3. CHEMICAL COMPOSITION OF MASUYITE

Point#	1	3	7	Av.	2	4	5	6	Av.
UO_3 wt.%	72.22	72.20	72.04	72.15	67.38	67.51	68.29	67.26	67.61
PbO	18.94	18.75	18.95	18.88	25.70	25.62	26.49	25.89	25.92
H_2O*	6.06	6.06	6.05	6.06					
Total	97.22	97.01	97.04	97.09					

* The proportion of H_2O is calculated on the basis of the structure determination.
# 1, 3, 7: core; 2, 4, 5, 6: rim

was done using standard ZAF techniques. The operating voltage was 15 kV, and the beam current was 20 μA. A beam 5 μm in diameter was employed to minimize damage to the sample. Data for all elements in the sample were collected for 30 s on the peak and 20 s on the background positions or 0.2% precision, whichever was attained first. Collection of a 100 s energy-dispersion spectrum did not reveal any elements other than Pb and U. Standards used for the electron-microprobe analysis were: synthetic UO_2 for U, and PbS for Pb. The proportion of H_2O was calculated by stoichiometry from the results of the crystal-structure analysis. Inspection of electron back-scatter images of the crystal showed that it is chemically zoned (see below); the location of each spot analyzed (Table 3) is shown in Figure 2.

Structure Solution and Refinement

Scattering curves for neutral atoms, together with anomalous dispersion corrections, were taken from *International Tables for X-Ray Crystallography, Vol. IV* (Ibers & Hamilton 1974). The Bruker SHELXTL Version 5 system of programs was used for the refinement of the structure.

Reflection statistics and systematic absences indicate the space group *Pn*, which was verified by the successful solution of the structure by direct methods. The initial model included the positions of the U and Pb atoms, and anions were located in difference-Fourier maps after least-squares refinement of the model. Following refinement of the atomic positional parameters and isotropic-displacement parameters for all atoms, the agreement factor (R) was 10.7% for observed reflections. Conversion of the cation displacement-parameters to an anisotropic form, together with refinement of the entire model, resulted in an R of 8.6%. A comparison of the observed structure-factors with those calculated using the model revealed that many F_{obs} were much greater than F_{calc}, indicating that the crystal may be twinned. The β angle is 90.402(4)°, suggesting that the twinning may involve inversion of the b and c axis. Allowing for this twinning using the method of Jameson (1982) and Herbst-Irmer & Sheldrick (1998), together with refinement of the entire model and a weighting scheme for the structure factors, provided a final R of 6.3% for the 2473 unique observed ($|F_o| \geq 4\sigma_F$) reflections and a goodness-of-fit (S) of 1.12. A model including anisotropic displacement of the anions was tried, but it did not lower the final R, and some of the resulting displacement parameters were found to be unrealistic. In the final cycle of refinement, the average parameter shift/esd was 0.000. The final atomic-position parameters and anisotropic-displacement parameters are given in Tables 4 and 5, and selected interatomic-distances and angles are given in Table 6. Calculated and observed structure-factors are available from the Depository of Unpublished Data, CISTI, National Research Council, Ottawa, Ontario K1A 0S2, Canada.

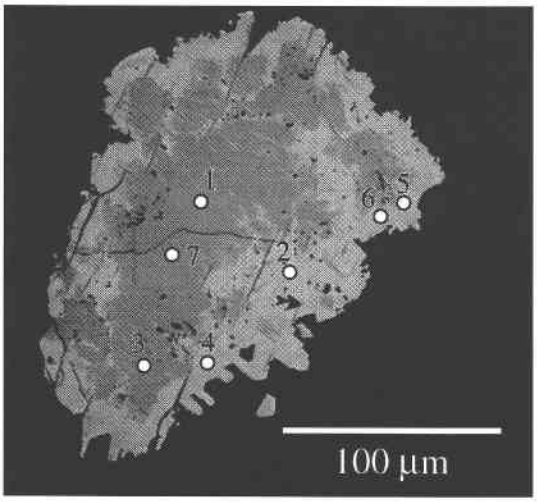

FIG. 2. Electron back-scatter image of the crystal of masuyite analyzed. The brighter regions correspond to higher mean atomic number.

Results of the Chemical Analysis

The electron back-scatter image (Fig. 2) clearly shows significant chemical variation in the crystal under study, and the analysis show that the core of the crystal (anal. 1, 3, 7) is relatively poor in Pb compared to

TABLE 4. ATOMIC POSITION PARAMETERS AND EQUIVALENT ISOTROPIC-DISPLACEMENT PARAMETERS FOR THE STRUCTURE OF MASUYITE

	x	*y*	*z*	$*U_{eq}$
U(1)	0.9988(1)	0.0185(1)	0.0024(2)	160(4)
U(2)	0.1797(1)	0.0180(1)	0.5419(2)	164(3)
U(3)	0.8802(1)	0.0122(1)	0.4836(2)	180(4)
Pb(1)[#]	0.0254(2)	0.4960(2)	0.6625(4)	328(8)
Pb(2)[#]	0.853(2)	0.509(2)	0.192(4)	415(74)
O(1)	0.994(3)	0.283(4)	0.029(6)	416(73)
O(2)	0.008(3)	0.767(4)	0.957(5)	377(77)
O(3)	0.196(3)	0.270(4)	0.496(5)	342(70)
O(4)	0.162(3)	0.763(4)	0.610(5)	360(70)
O(5)	0.868(3)	0.271(4)	0.451(4)	316(61)
O(6)	0.895(2)	0.756(4)	0.536(4)	361(65)
O(7)	0.018(3)	0.086(4)	0.681(4)	370(63)
O(8)	0.041(5)	0.974(5)	0.302(9)	648(139)
O(9)	0.847(2)	0.984(2)	0.174(4)	101(44)
OH(10)	0.194(3)	0.053(4)	0.924(5)	329(58)
OH(11)	0.812(3)	0.065(5)	0.787(5)	403(68)
H_2O(12)	0.802(5)	0.485(5)	0.832(9)	536(123)
H_2O(13)	0.190(3)	0.482(3)	0.938(4)	160(49)
H_2O(14)	0.061(2)	0.525(3)	0.296(5)	204(56)

$*U_{eq} = U_{eq}$ Å^2 x 10^4

[#]refined occupancy factors for Pb(1) = 0.93(1) and Pb(2) = 0.12(2)

TABLE 5. ANISOTROPIC-DISPLACEMENT PARAMETERS FOR THE CATIONS IN THE STRUCTURE OF MASUYITE

	$*U_{11}$	U_{22}	U_{33}	U_{12}	U_{13}	U_{23}
U(1)	136(6)	290(6)	53(6)	35(9)	-33(6)	-35(11)
U(2)	59(6)	247(6)	185(8)	55(9)	10(6)	14(10)
U(3)	116(6)	262(6)	163(8)	27(7)	20(5)	-22(8)
Pb(1)	331(13)	300(9)	352(14)	9(6)	8(10)	36(6)

$*U_{ij} = U_{ij}$ Å^2 x 10^4

TABLE 6. SELECTED INTERATOMIC DISTANCES (Å) AND ANGLES (°) IN THE STRUCTURE OF MASUYITE

U(1)-O(2)a	1.80(3)	U(2)-O(3)	1.81(3)
U(1)-O(1)	1.86(3)	U(2)-O(4)c	1.86(3)
U(1)-O(8)b	2.18(6)	U(2)-O(9)f	2.24(3)
U(1)-O(9)c	2.23(3)	U(2)-O(7)	2.26(3)
U(1)-O(7)d	2.31(3)	U(2)-O(8)c	2.39(6)
U(1)-OH(10)d	2.47(3)	U(2)-OH(11)g	2.49(3)
U(1)-OH(11)e	2.74(3)	U(2)-OH(10)	2.68(3)
<U-O_{Ur}>	1.83	<U-O_{Ur}>	1.84
<U-ϕ_{eq}>	2.39	<U-ϕ_{eq}>	2.41
O(2)a-U(1)-O(1)	175(2)	O(3)-U(2)-O(4)c	175(1)
U(3)-O(5)	1.84(3)	Pb(1)-O(4)	2.54(3)
U(3)-O(6)c	1.84(2)	Pb(1)-O(6)j	2.57(3)
U(3)-O(9)c	2.21(3)	Pb(1)-H_2O(14)	2.61(3)
U(3)-O(7)h	2.23(3)	Pb(1)-H_2O(13)	2.77(3)
U(3)-OH(11)	2.31(3)	Pb(1)-O(2)	2.81(3)
U(3)-OH(10)i	2.36(3)	Pb(1)-O(3)	2.87(3)
U(3)-O(8)b	2.37(6)	Pb(1)-O(7)	2.88(3)
<U-O_{Ur}>	1.84	Pb(1)-O(5)j	2.89(3)
<U-ϕ_{eq}>	2.30	Pb(1)-H_2O(12)j	2.99(6)
O(5)-U(3)-O(6)c	175(1)	Pb(1)-O(1)k	2.99(4)
		<Pb(1)-ϕ>	2.79
Pb(2)-O(5)	2.46(4)		
Pb(2)-H_2O(12)e	2.59(6)		
Pb(2)-O(1)	2.61(4)	a = x+1, y-1, z-1; b = x+1, y-1, z;	
Pb(2)-H_2O(14)h	2.64(4)	c = x, y-1, z; d = x+1, y, z-1; e = x,	
Pb(2)-H_2O(13)l	2.65(4)	y, z-1; f = x-½, 1-y, z+½; g = x-½,	
Pb(2)-O(3)l	2.82(4)	-y, z-½; h = x+1, y, z; i = x+½; -y,	
Pb(2)-O(6)	3.00(4)	z-½; j = x-1, y, z; k = x-1, y, z+1;	
Pb(2)-O(4)l	3.07(4)	l = x+½, 1-y, z-½	
Pb(2)-O(2)d	3.10(4)		
<Pb(2)-ϕ>	2.77		

the rim (anal. 2, 4, 5, 6, Table 3). The mottled appearance of the zoning suggests that the crystal originally grew with a composition similar to that found in the core, followed by interaction with fluids that were richer in Pb, causing alteration of the outer portions of the crystal. This is consistent with the lower mobility of Pb than of U^{6+} in solution (Mann & Deutscher 1980); as alteration of uraninite advances, the paragenetic sequence of Pb uranyl oxide hydrate minerals typically involves a continued increase in Pb:U ratio (Finch & Ewing 1992b).

The formula derived from the chemical analysis done near the core of the crystal is $Pb_{1.01}[(UO_2)_3O_3(OH)_2](H_2O)_3$, with the amount of H_2O assumed on the basis of the crystal-structure determination (see below). The Pb:U ratio of ~1:3 is consistent with this being the Pb analogue of protasite, "masuyite I" as reported by Finch & Ewing (1992b), and "grooved masuyite" reported by Deliens & Piret (1996). The analysis carried out on the outer portions of the crystal gave a Pb:U ratio of ~1:2, which is even more Pb-rich than "masuyite II"

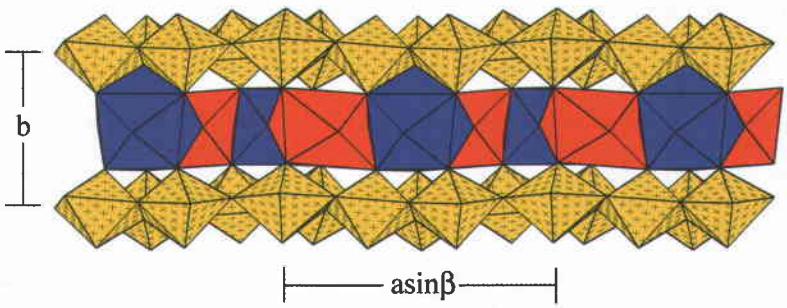

FIG. 3. The structure of masuyite projected along [001]. The uranyl polyhedra are shown in yellow, the Pb(1) polyhedra in blue, and the Pb(2) polyhedra in red.

TABLE 7. BOND-VALENCE ANALYSIS* (*vu*) FOR THE STRUCTURE OF MASUYITE

	U(1)	U(2)	U(3)	Pb(1)	Pb(2)	Σ#
O(1)	1.44			0.09	0.26	1.55
O(2)	1.62			0.15	0.07	1.77
O(3)		1.59		0.13	0.15	1.73
O(4)		1.44		0.31	0.08	1.74
O(5)			1.49	0.12	0.39	1.65
O(6)			1.49	0.29	0.09	1.77
O(7)	0.59	0.66	0.70	0.13		2.07
O(8)	0.77	0.52	0.53			1.81
O(9)	0.70	0.68	0.72			2.10
OH(10)	0.43	0.29	0.54			1.26
OH(11)	0.26	0.42	0.59			1.27
H_2O(12)				0.09	0.27	0.12
H_2O(13)				0.17	0.23	0.19
H_2O(14)				0.26	0.24	0.27
Σ	5.80	5.58	6.07	1.75	1.78	

* bond-valence parameters for U^{6+} from Burns *et al.* (1997) and for Pb^{2+} from Brese & O'Keeffe (1991)
# bond-valence contributions into the anion sums from Pb-ϕ bonds have been scaled by the partial occupancy of each Pb site

of Finch & Ewing (1992b), and is close to that of wölsendorfite (Table 1; Burns 1999). Note that effects of chemical zonation were not observed in the single-crystal diffraction data. The crystal used for the structure determination was a fragment, and probably corresponded to the inner portion of a larger crystal.

Description of the Structure

The structure is shown projected along [001] in Figure 3. As is the case for each of the other Pb uranyl oxide hydrate minerals, the structure is composed of sheets of uranyl polyhedra, with the Pb cations and H_2O groups located in the interlayer.

Cation polyhedra

The structure contains three symmetrically distinct U cations, each of which is strongly bonded to two O atoms with bond-lengths of ~1.8 Å, forming approximately linear $(UO_2)^{2+}$ uranyl ions (*Ur*). The <U–O_{Ur}> bond-lengths range from 1.82 to 1.84 Å, values that compare well with the average uranyl ion bond-length of 1.79(4) for $^{[7]}U^{6+}$ in numerous well-refined structures (Burns *et al.* 1997). The U cations are each coordinated by three additional atoms of O and two $(OH)^-$ groups arranged at the equatorial corners of pentagonal bipyramids, with the O_{Ur} atoms capping the bipyramids. The pentagonal bipyramid is the most common uranyl polyhedron in minerals (Evans 1963, Burns *et al.* 1997). The <U–ϕ_{eq}> bond-lengths range from 2.30 to 2.41 Å, comparable to the value of 2.37(9) Å obtained for uranyl pentagonal bipyramids in numerous well-refined structures (Burns *et al.* 1997). The polyhedron geometries and bond-valence sums incident at the U positions (Tables 6, 7) are consistent with each site containing U^{6+}.

The structure contains two partially occupied Pb^{2+} sites in the interlayer; partial occupancy of the Pb sites is common in other Pb uranyl oxide hydrates. The structure refinement gave Pb(1) and Pb(2) site-occupancy factors of 0.93(1) and 0.12(2). The Pb(1) site is coordinated by seven atoms of O and three H_2O groups, with a <Pb–ϕ> bond-length of 2.79 Å. The polyhedron includes six O_{Ur} atoms of adjacent sheets of uranyl polyhedra, as well as one O atom located at the equatorial positions of three uranyl pentagonal bipyramids. The Pb(2) site is coordinated by six O_{Ur} atoms and three H_2O groups, with an <Pb–ϕ> bond-length of 2.77 Å.

Sheets of uranyl polyhedra

The uranyl pentagonal bipyramids share edges and corners, forming sheets that are parallel to (010) (Fig. 4). This sheet is well known from other uranyl minerals, and is generally referred to as the α-U_3O_8-type or protasite-type sheet (Burns *et al.* 1996). Topologically identical sheets occur in the structures of protasite (Pagoaga *et al.* 1987), compreignacite (Burns 1998c), billietite (Pagoaga *et al.* 1987), becquerelite (Pagoaga *et al.* 1987), richetite (Burns 1998b), and a synthetic Cs uranyl oxide hydrate (Hill & Burns 1999). However, the distribution of anions is not identical in these sheets, and four distinct arrangements are known (Hill & Burns 1999). The anion topology of the masuyite sheet is shown in Figure 5, with each $(OH)^-$ group designated by an open circle. The distribution of $(OH)^-$ within the anion topology is identical to that in the sheets that occur in protasite.

Interlayer connectivity

The interlayer of the structure is shown projected along [010] in Figure 6. The Pb(1) polyhedra, which are close to being fully occupied, do not share polyhedron elements with other Pb(1) polyhedra. However, each Pb(1) polyhedron shares three of its faces with the low-occupancy Pb(2) polyhedra, and each Pb(2) polyhedron shares faces with three Pb(1) polyhedra, forming sheets of Pb polyhedra that are parallel to (010). Separation of adjacent Pb(1) and Pb(2) cations are 3.89, 4.02 and 4.27 Å; thus it is possible for both of the Pb(1) and Pb(2) polyhedra to be occupied locally.

Formula of the crystal studied

All atoms in the structure are on general positions in space group *Pn* (Table 4). The polyhedron geometries and bond-valence sums indicate that all three U sites contain U^{6+}, the total occupancy of the Pb(1) and Pb(2) sites is 1.05, and the bond-valence analysis (Table 7) indicates that there are nine O, two $(OH)^-$ and three H_2O sites. Therefore, the ideal structural formula of the crystal studied is $Pb[(UO_2)_3O_3(OH)_2](H_2O)_3$. This formula

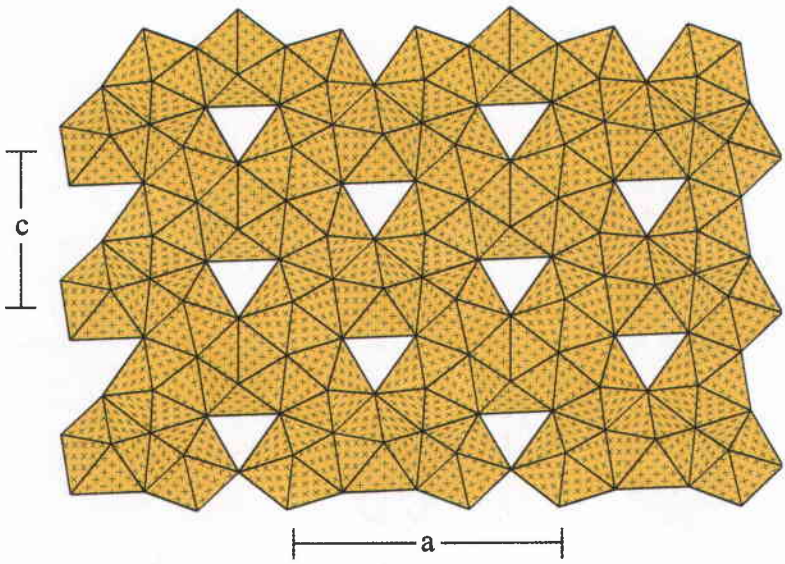

FIG. 4. The sheet of uranyl polyhedra in the structure of masuyite shown projected along [010].

is in excellent agreement with that obtained from the chemical analysis of the core of the crystal studied.

RELATIONSHIP TO PROTASITE

The structure determination has shown that the structure of the crystal of masuyite studied is closely related to that of protasite (Pagoaga *et al.* 1987). The sheets of uranyl polyhedra, including the distribution of anions within the anion topology, are identical in the two minerals. The interlayers contain the same number of H_2O groups, and the Pb(1) site in masuyite is comparable to the Ba site in protasite. However, the structures differ owing to the presence of the Pb(2) site in masuyite; there is no corresponding site in the structure of protasite.

The structure of richetite (Burns 1998b) also contains a α-U_3O_8-type sheet (Fig. 1d); it is topologically identical to the sheet found in masuyite, but the distribution of anions within the two corresponding sheet anion-topologies is distinct.

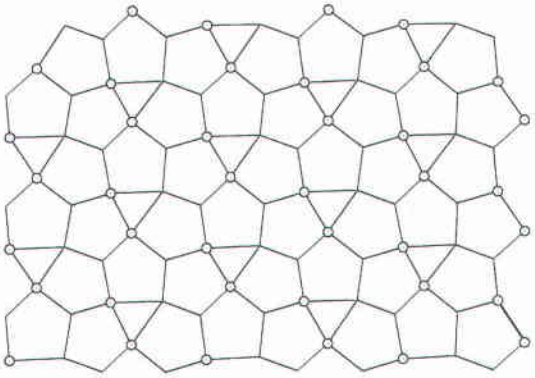

FIG. 5. The sheet anion-topology of the sheet of uranyl polyhedra in masuyite, derived using the method of Burns *et al.* (1996). The location of $(OH)^-$ groups is shown by circles.

Pb VARIABILITY IN MASUYITE

The Pb(2) site in the crystal studied is only 12% occupied, although there is no geometrical requirement that the occupancy remain low. Is it possible that a series of masuyite crystals exists with Pb contents that are higher than those found in the crystal under study? Modification of the interlayer Pb occupancy requires a charge-balance mechanism. Assuming the formula $[(UO_2)_3O_3(OH)_2]$ for the sheet, and no charged species other than Pb in the interlayer of the structure, electroneutrality requires one atom of Pb per formula unit, as is approximately the case in the crystal of the current study. Variability of the Pb content must either involve a change in the net charge of the sheet of polyhedra, or the inclusion of a charged species in the interlayer, such as $(OH)^-$.

Modification of the charge of the sheet may be achieved by the substitution $O^{2-} \leftrightarrow (OH)^-$. Sheets with identical anion-topologies as the masuyite sheet occur in several structures, with various distributions of $(OH)^-$

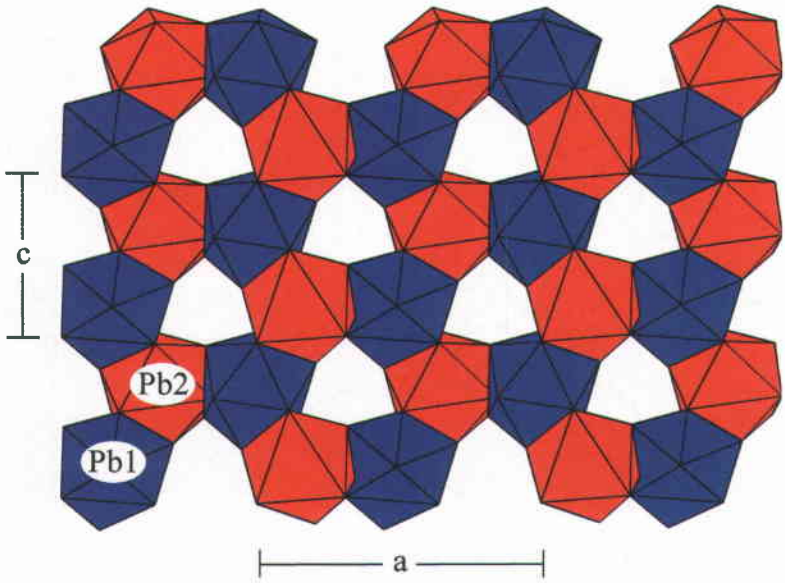

FIG. 6. The interlayer of the structure of masuyite projected along [010].

over the nodes of the anion topology. However, no uranyl minerals with structures based upon the protasite anion-topology are known that have a lower hydration state than those of masuyite and protasite, possibly indicating that a lower-hydrate sheet would be unstable. Additional structural studies are required to elucidate the structural mechanism of Pb variability in masuyite.

ACKNOWLEDGEMENTS

The crystal used in this study, as well as many other specimens of uranyl minerals, was provided by the Canadian Museum of Nature. This research was funded by the National Science Foundation (EAR98–04723). Thanks to Yves Thibault at the University of Western Ontario for his assistance with the electron-microprobe analysis. The manuscript was improved following reviews by Drs. C.M. Gramaccioli and R. Vochten, as well as editorial work by R.F. Martin.

REFERENCES

BRASSEUR, H. (1950): Etude roentgenographique de la masuyite. *Bull. Soc. R. Sci. Liège* **19**, 239.

BRESE, N.E. & O'KEEFFE, M. (1991): Bond-valence parameters for solids. *Acta Crystallogr.* **B47**, 192-197.

BURNS, P.C. (1997): A new uranyl oxide hydrate sheet in the structure of vandendriesscheite: implications for mineral paragenesis and the corrosion of spent nuclear fuel. *Am. Mineral.* **82**, 1176- 1186.

_____ (1998a): CCD area detectors of X-rays applied to the analysis of mineral structures. *Can. Mineral.* **36**, 847-853.

_____ (1998b): The structure of richetite, a rare lead uranyl oxide hydrate. *Can. Mineral.* **36**, 187-199.

_____ (1998c): The structure of compreignacite, $K_2[(UO_2)_3O_2(OH)_3]_2(H_2O)_7$. *Can. Mineral.* **36**, 1061-1067.

_____ (1999): A new complex sheet of uranyl polyhedra in the structure of wölsendorfite. *Am. Mineral.* **84**, 1661-1673.

_____, EWING, R.C. & HAWTHORNE, F.C. (1997): The crystal chemistry of hexavalent uranium: polyhedron geometries, bond-valence parameters, and polymerization of polyhedra. *Can. Mineral.* **35**, 1551-1570.

_____ & HILL, F.C. (2000): Implications of the synthesis and structure of the Sr analogue of curite. *Can. Mineral.* **38** (in press).

_____, MILLER, M.L. & EWING, R.C. (1996): U^{6+} minerals and inorganic phases: a comparison and hierarchy of crystal structures. *Can. Mineral.* **34**, 845-880.

CHRIST, C.L. & CLARK, J.R. (1960): Crystal chemical studies of some uranyl oxide hydrates. *Am. Mineral.* **45**, 1026-1061.

DELIENS, M. & PIRET, P. (1996): Les masuyites de Shinkolobwe (Shaba, Zaïre) constituent un groupe formé de deux variétés distinctes par leur composition chimique et leurs propriétés radiocristallographiques. *Bull. Inst. R. Sci. Natur. Belgique, Sci. Terre* **66**, 187-192.

_____, _____ & COMPLAIN, G. (1981): *Les Minéraux Secondaires d'Uranium du Zaïre*. Musée Royal de l'Afrique Centrale, Tervuren, Belgique.

EVANS, H.T., JR. (1963): Uranyl ion coordination. *Science* **141**, 154-157.

FINCH, R.J., COOPER, M.A. & HAWTHORNE, F.C. (1996): The crystal structure of schoepite, $[(UO_2)_8O_2(OH)_{12}](H_2O)_{12}$. *Can. Mineral.* **34**, 1071-1088.

_____ & EWING, R.C. (1991): Phase relations of the uranyl oxide hydrates and their relevance to the disposal of spent fuel. *Mat. Res. Soc., Symp. Proc.* **212**, 241-246.

_____ & _____ (1992a): Alteration of natural uranyl oxide hydrates in Si-rich groundwaters: implications for uranium solubility. *Mat. Res. Soc., Symp. Proc.* **257**, 465-472.

_____ & _____ (1992b): The corrosion of uraninite under oxidizing conditions. *J. Nucl. Mater.* **190**, 133-156.

FRONDEL, C. (1958): Systematic mineralogy of uranium and thorium. *U.S. Geol. Surv., Bull.* **1064**.

HERBST-IRMER, R. & SHELDRICK, G.M. (1998): Refinement of twinned structures with SHELXL97. *Acta Crystallogr.* **B54**, 443-449.

HILL, F.C. & BURNS, P.C. (1999): The structure of a synthetic Cs uranyl oxide hydrate and its relationship to compreignacite. *Can. Mineral.* **37**, 1283-1288.

IBERS, J.A. & HAMILTON, W.C., eds. (1974): *International Tables for X-ray Crystallography* **IV**. The Kynoch Press, Birmingham, U.K.

JAMESON, G.B. (1982): On structure refinement using data from a twinned crystal. *Acta Crystallogr.* **A38**, 817.

KOVBA, L.M. (1972): Crystal structure of $K_2U_7O_{22}$. *J. Struct. Chem.* **13**, 235-238.

MANN, A.W. & DEUTSCHER, R.L. (1980): Solution chemistry of lead and zinc in water containing carbonate, sulphate and chloride ions. *Chem. Geol.* **29**, 293-311.

PAGOAGA, M.K., APPLEMAN, D.E. & STEWART, J.M. (1987): Crystal structures and crystal chemistry of the uranyl oxide hydrates becquerelite, billietite, and protasite. *Am. Mineral.* **72**, 1230-1238.

PIRET, P. (1985): Structure cristalline de la fourmariérite, $Pb(UO_2)_4O_3(OH)_4 \cdot 4H_2O$. *Bull. Minéral.* **108**, 659-665.

_____, DELIENS, M., PIRET-MEUNIER, J. & GERMAIN, G. (1983): La sayrite, $Pb_2[(UO_2)_5O_6(OH)_2] \cdot 4H_2O$, nouveau minéral; propriétés et structure cristalline. *Bull. Minéral.* **106**, 299-304.

TAYLOR, J.C., STUART, W.L. & MUMME, I.A. (1981): The crystal structure of curite. *J. Inorg. Nucl. Chem.* **43**, 2419-2423.

VAES, J.F. (1947): Six nouveaux minéraux d'urane provenant de Shinkolobwe (Katanga). *Ann. Soc. Géol. Belgique* **70**, B212-B226.

Received February 28, 1999, revised manuscript accepted December 12, 1999.